

PCCP

Accepted Manuscript



This is an *Accepted Manuscript*, which has been through the Royal Society of Chemistry peer review process and has been accepted for publication.

Accepted Manuscripts are published online shortly after acceptance, before technical editing, formatting and proof reading. Using this free service, authors can make their results available to the community, in citable form, before we publish the edited article. We will replace this *Accepted Manuscript* with the edited and formatted *Advance Article* as soon as it is available.

You can find more information about *Accepted Manuscripts* in the [Information for Authors](#).

Please note that technical editing may introduce minor changes to the text and/or graphics, which may alter content. The journal's standard [Terms & Conditions](#) and the [Ethical guidelines](#) still apply. In no event shall the Royal Society of Chemistry be held responsible for any errors or omissions in this *Accepted Manuscript* or any consequences arising from the use of any information it contains.

Anion states and fragmentation of 2-chloroadenine upon low-energy electron collisions

F. Kossoski,¹ J. Kopyra,² and M. T. do N. Varella¹

¹*Instituto de Física, Universidade de São Paulo, Caixa Postal 66318, 05314-970, São Paulo, São Paulo, Brazil*

²*Siedlce University, Faculty of Science, 3 Maja 54, 08-110 Siedlce, Poland*

We report on a joint theoretical and experimental investigation on the electron-induced fragmentation of 2-chloroadenine, for electrons up to 12 eV. Elastic scattering calculations indicate an anion spectra comprising a σ_{CCl}^* and four π^* shape resonances, where the latter are systematically stabilised when compared to the analogue states of adenine. The measured ion yields indicate strong signals associated with elimination of neutral hydrogen (peaking at 0.8 eV and with milder structures up to 2 eV), chloride ion and hydrochloric acid (both observed around 0.2 and 0.9 eV). Bound state calculations indicate the main feature for hydrogen abstraction arises from a vibrational Feshbach resonance on a dipole-bound state coupled to a σ_{NH}^* state, while the π_2^* and π_3^* resonances initiate this fragmentation process in the 1–2 eV region. On the other hand, the C–Cl bond cleavage would mainly arise from the formation of the π_1^* and π_2^* resonances, which couple to the dissociative σ_{CCl}^* state. Our results show that 2-chloroadenine efficiently dissociates into reactive species upon electron attachment, corroborating its potential as a radiosensitising drug.

PACS numbers: 34.80.Bm, 34.80.Gs

I. INTRODUCTION

Radiosensitisers are molecules with the ability to enhance the biological damage when exposed to ionising radiation. In the biological medium, the incident radiation gives rise to secondary species, the most abundant being pre-hydrated electrons that thermalise in a picosecond time scale. The secondary species actually account for most of the damage to the biomolecules, and may cause DNA strand breaks leading to genotoxic and carcinogenic effects.¹ However, these electron-induced fragmentation processes, often referred to as dissociative electron attachment (DEA)², can become beneficial in case they induce the dissociation of radiosensitising drugs. These chemicals are designed to either replace a natural nucleoside (metabolite) or bind to its structure. Dissociation, apart from bond rupture leading to the formation of fragment anions, can also produce reactive radicals that subsequently attack the DNA strands (free radical damage³). A slow electron can be captured into an empty molecular orbital, thus forming a transient negative ion (shape resonance). This anion state quickly releases the electron energy into vibrational degrees of freedom, possibly leading to bond breaking and/or significant vibrational excitation. The competition between vibrational relaxation and electron detachment governs the DEA cross sections, which ultimately could correlate to the radiosensitivity of the molecule.

It is therefore of vital importance to comprehend the interaction of electrons with biomolecules and how the subsequent DEA processes take place. While many studies have addressed pyrimidine nucleobase derivatives, purine derivatives have only received more attention in recent years. Theoretical studies on brominated purines support the prompt stabilisation through bromide elimination.⁴⁻⁷ For 8-bromoadenine⁵ and 8-bromoguanine⁶ nucleotides, the radical nucleobases would trigger reactions leading to the phosphodiester cleavage, and hence to DNA strand breaks. Experiments on electron collisions with films of nucleotide trimers⁸ have confirmed the ability of bromopurines to produce biological damage, and it has been suggested that it could be even larger compared to pyrimidine analogues.^{7,8}

In spite of the growing interest on new radiosensitising molecules and the recent findings on halogenated purines, the available information on electron interactions with this class of molecules, in particular the mechanisms underlying its bioactivity, is sketchy at present. Aiming at partially filling this gap, we report theoretical and experimental results on the

fragmentation of gas-phase 2-chloroadenine. On the theory side, we investigate the transient anion states that could trigger DEA processes, while the experimental data points out the ion yields. The comparison between theory and experiment can therefore indicate the mechanisms connecting electron attachment with the dissociation products (to our knowledge there are no reported studies on low-energy electron collisions for this molecule). We also report calculations for adenine for comparison with 2-chloroadenine and with previous calculations⁹⁻¹¹ (systematically overestimated with respect to the observed resonance energies¹²).

II. COMPUTATIONAL PROCEDURES

The fixed-nuclei scattering calculations were performed at the equilibrium geometry of the target ground state as obtained from Density Function Theory (DFT) with the hybrid B3LYP functional and the 6-311++G(2d,1p) basis set. The target ground state was described at the restricted Hartree-Fock (HF) level, with Cartesian Gaussian functions generated according to Bettega *et al.*¹³ We employed a 5s5p2d basis set for carbon, nitrogen and chlorine (with the same exponents given in Ref.¹⁴), and the 3s basis set of Dunning, Jr.¹⁵ for hydrogen. In both bound state and scattering calculations norm-conserving pseudopotentials of Bachelet, Hamann and Schlüter (BHS)¹⁶ were used to represent the nuclei and core electrons of all atoms except for hydrogen. For geometry optimisations and target ground state descriptions we employed the Gamess package.¹⁷

The elastic cross sections were computed with the Schwinger multichannel method (SMC)¹⁸ implemented with pseudopotentials (SMCPP)¹⁹ and parallel processing²⁰ (see Ref.²¹ for a review). Here we limit the discussion to the relevant aspects concerning the present application. The scattering wavefunction is expanded in a set of configuration state functions (CSFs) $\{|\chi_m\rangle\}$, given by products of target states and single-particle functions (scattering orbitals). The calculations were performed in the static-exchange (SE) approximation, wherein the target electronic cloud is kept frozen in the ground state, and the static-exchange plus polarisation (SEP) approximation, which takes into account the dynamical response of the target due to the incoming electron. In the former level of approximation, the CSFs were generated as $|\chi_j\rangle = A[|\Phi_0\rangle \otimes |\varphi_j\rangle]$, while in the latter the CSF space is augmented with configurations built as $|\chi_{ij}\rangle = A[|\Phi_i\rangle \otimes |\varphi_j\rangle]$, where $|\Phi_0\rangle$ is the target

ground state, $|\Phi_i\rangle$ is a singly-excited virtual target state, $|\varphi_j\rangle$ is the scattering orbital and A is the antisymmetriser. The set of $|\Phi_i\rangle$ target functions were described as single virtual excitations from hole to particle orbitals. Instead of the canonical HF virtual orbitals, we employed modified virtual orbitals (MVOs)²² to represent particle and scattering orbitals, as generated in the field of the cation with charge +6.

Although 2-chloroadenine is not strictly planar due to the pyramidisation of the C–NH₂ group, the deviation from planarity is very minor, as in adenine²³. For both 2-chloroadenine and adenine, we reoptimised the molecular geometry imposing the C_s symmetry, and performed the scattering calculations with this constraint, as in Refs.^{10,11}. While having only a minor impact on the resonance positions, this procedure allows for the symmetry decomposition of the calculated cross sections, which reduces the computational effort and facilitates the assignment of the anion state characters as π^* or σ^* . For both molecules, the calculations were performed separately for the A' and A'' symmetry components, and the CSF spaces were built from the energy criterion²⁴ $\varepsilon_{scat} + \varepsilon_{part} - \varepsilon_{hole} < \varepsilon_{cut}$, where ε_{scat} , ε_{part} and ε_{hole} are the energies of the scattering, particle and hole orbitals, respectively, and ε_{cut} is an energy threshold. We employed $\varepsilon_{cut} = -1.09$ Hartree and allowed for singlet- and triplet-coupled target excitations (while keeping only the doublets in the scattering wave function expansion), giving rise to 26 223 CSFs for 2-chloroadenine (13 052 configurations in the A' and 13 171 in the A'' symmetry components) and 25 371 for adenine (12 604 in the A' and 12 767 in the A'' components).

In the present calculations the high partial waves are not corrected to account for the long-range dipole potential contribution (Born closure). This contribution would essentially increase the background magnitude and make the signature of the resonance states less clear²⁵. Since we are interested in calculating the shape resonance spectra, described by the lower partial waves, we report uncorrected cross sections, with underestimated magnitudes, to highlight the anion state signatures. The resonances positions and widths were obtained from least-square fits of the computed eigenphase sums to a functional form comprising the Breit-Wigner profile and a second-order degree polynomial to describe the background.

The significant dipole moment magnitude of 2-chloroadenine, 4.1 D at the DFT/B3LYP/6-311++G(2d,1p) level, would be expected to give rise to a dipole bound state (DBS). In order to describe this state, we performed independent bound state calculations with the Gaussian09 software.²⁶ We employed the aug-cc-pVDZ basis set augmented with a set of

6s6p diffuse functions located on the hydrogen bonded to the nitrogen atom in the imidazole ring, which lies close to the positive pole of the molecule. The exponents of the extra set were chosen in an even-tempered fashion,²⁷ through successive divisions by 4, starting from the most diffuse hydrogen exponent in the aug-cc-pVDZ set. The optimised neutral ground state and vibrational frequencies were obtained from Møller-Plesset second-order perturbation theory (MP2), while electronic correlation was incorporated with MP2 and coupled-cluster with single, double and perturbative triple excitations (CCSD(T)) for both neutral and anion states. Finally, the dissociation thresholds were computed with the composite G4(MP2) method, also employing the Gaussian09 software.

III. EXPERIMENTAL PROCEDURE

The experiments are performed in a crossed-beam arrangement consisting of an electron source, an oven and a quadrupole mass analyzer (QMA). The components are housed in a UHV chamber at a base pressure of 10^{-9} mbar. A well-defined electron beam generated from a trochoidal electron monochromator (≈ 250 meV FWHM, electron current around 10 nA), orthogonally intersects with an effusive molecular beam of 2-chloroadenine (97% purity powder, purchased from Sigma Aldrich). The molecular beam emanates from the vessel heated by two in vacuo halogen bulbs. In the present work, the material was heated up to 443 K, as measured by a platinum resistance mounted at one of the flanges. Since our experimental temperature is well below the melting temperature (657–662 K), the evaporated molecules are likely to remain intact. Negative ions that are generated in the reaction area due to collision of electrons with intact molecules, are extracted from the interaction area towards the QMA and detected by single pulse counting techniques. The electron energy scale is calibrated by using the SF₆ gas yielding the well-known SF₆⁻ resonance near zero eV. However, the measurements are performed without the presence of the calibration gas in order to avoid unwanted reactions such as dissociative electron transfer.

IV. RESULTS AND DISCUSSION

The elastic integral cross sections (ICSs) of 2-chloroadenine, computed in both SE and SEP approximations, are shown in Fig. 1. In the A'' symmetry component, there are four

prominent peaks in the ICSs curves, which are signatures of π^* shape resonances. These are hereafter labelled π_1^* , π_2^* , π_3^* and π_4^* from the lowest- to the highest-lying. To gain insight into the character of the anion states, we show in Fig. 2 virtual orbitals obtained with the 6-31G(d) compact basis set. In the lower-level SE calculations, the resonances are located at 2.61, 3.43, 4.6 and 9.8 eV, while the more accurate SEP calculations place them at 0.29, 0.73, 2.55 and 5.69 eV. The four π^* anion states would be shape resonances, as they appear in the SE calculations. However, the thresholds for excitation of triplet and singlet electronic states of adenine would be around 3.6 eV and 5.0 eV, respectively²⁸, pointing out that the π_4^* anion state of 2-chloroadenine should lie well into the electronic excitation region. The position of resonances lying close to the threshold for triplet excitations are usually overestimated in elastic calculations (neglecting electronic excitation channels) by 0.5–1 eV, as these anion states develop a mixed shape and core-excited character.^{29,30} The π_4^* resonance of 2-chloroadenine would be expected to correlate to core-excited states (neglected in the present work) and its position, as obtained from the present elastic calculations, would be subjected to significant error. We also performed exploratory configuration interaction calculations to inspect the character of the π_3^* resonance. These studies support the assignment of the three lowest-lying π^* anion states as shape resonances. In the SEP approximation the ICSs present zigzag patterns above ~ 6.5 eV, which arise from (unphysical) pseudoresonances³¹.

The A' component of the ICS presents a structure around 6 eV in the SE calculation that is displaced to 3.3 eV when polarisation effects are accounted for. We assign this peak to a σ_{CCl}^* shape resonance, arising from electron capture into the anti-bonding orbital located at the C–Cl bond (see Fig. 2). In view of the significant background contribution, the eigenphase fit provides a resonance energy (3.00 eV) somewhat displaced from the peak maximum (3.3 eV). Since the eigenphase model employed in the least-squares fit properly incorporates the resonant and background components, this procedure is more reliable than simply inspecting the peak position. We also found broad structures around 11 and 16 eV in the SE results, which arise from overlapping short-lived σ^* shape resonances. In the SEP approximation, we cannot resolve the structures in the A' symmetry, due to the presence of pseudoresonances³¹, and only a broad structure around 8 eV is discernible. Furthermore, based on virtual orbital analysis (see below) and results for other systems,^{24,32} there might be a low-lying σ_{NH}^* shape resonance, associated with occupation of the anti-bonding orbital at the N–H bond of the imidazole ring (see Fig. 2). However, the expected large width

combined with the strong background scattering would be expected to obscure its signature in the ICS.^{20,33}

The computed elastic ICSs of adenine, in both SE and SEP approximations, are presented in Fig. 3. In agreement with previous reports,^{9–12} we also found four π^* shape resonances around 2.93, 3.77, 4.9 and 10.2 eV, in consistency with the positions obtained by Winstead and McKoy¹⁰ and by Dora *et al.*¹¹ Inclusion of polarisation effects brings the resonant peaks to lower energies, namely 0.56, 1.12, 2.72 and 6.02 eV. For the three lower-lying π^* resonances, our results agree well with the electron transmission (ET) measurements of Aflatooni *et al.*¹², 0.54, 1.36 and 2.17 eV. Tab. I summarises the positions and widths of the four π^* resonances of adenine, and it is noteworthy that we provide an overall good agreement with experiment. Winstead and McKoy¹⁰ showed for guanine, extending the argument to adenine, that once the planarity constraint is removed, the π^* resonances are stabilised by about 0.2 eV. That consideration would slightly improve our agreement for the two higher-lying π^* states, whereas the π_1^* and π_2^* resonances would be placed below the experimental value. As for the π_4^* state, we expect to be overestimating its energy by 0.5–1 eV, for the same reason as described for 2-chloroadenine, and thus it would locate around 5.0–5.5 eV. This resonance could give rise to very complex reactions, given the series of fragments observed in the DEA spectra in this region.³⁴

The A' ICS of adenine presents two higher-lying structures in the SE approximation, around 11 and 15 eV. Only a broad structure centered around 8 eV remains discernible when polarisation effects are included. Our result is similar to the previous SMC SE calculation,¹⁰ as well as the R-matrix SEP calculation.¹¹ Finally, a σ_{NH}^* shape resonance should also exist in adenine, but its short lifetime makes it hard to be identified, either theoretically or experimentally.

Now we move on to the comparison between the anion spectra of adenine and its chlorinated derivative. In order to help in the interpretation of the results, we present in Fig. 2 the HF virtual orbitals of 2-chloroadenine, as obtained with the 6-31G(d) basis set, with the geometry optimised at the MP2 level and same basis set, while restricting the molecule to the C_s point group. The lowest unoccupied molecular orbital (LUMO), LUMO+1, LUMO+2 and LUMO+9 represent the four π^* orbitals, while LUMO+3 and LUMO+4 correspond to the σ_{NH}^* and σ_{CCl}^* orbitals, respectively. Except for the σ_{CCl}^* orbital, all the others present very similar analogues in adenine. According to our scattering calculations, the π^* anion

states of 2-chloroadenine lie systematically below the corresponding states of adenine, due to the stabilising effect of the chlorine atom. Based on the orbitals character, one would expect this inductive stabilising effect to be more active on the π_2^* and π_4^* states (where the orbitals lie mostly on the pyrimidine ring, closer to chlorine), to have a minor influence on the π_3^* state (where the orbital locates at the farther imidazole ring), and an intermediate effect on the π_1^* state (orbital is spread in both rings). This reasoning is consistent with the observed behaviour on the π^* resonances upon chlorination, which are stabilised by 0.27, 0.39, 0.17 and 0.36 eV, as one moves from π_1^* to π_4^* .

The virtual orbitals also allow for estimates of vertical attachment energies (VAEs), based on empirical equations that relate them to the computed virtual orbital energies (VOEs). For the π^* states of 2-chloroadenine we employed the relation $\text{VAE} = 0.64795 \times \text{VOE} - 1.4298$ (in units of eV),³⁵ which provides 0.61, 1.12, 2.01 and 5.04 eV for their energies, in reasonable agreement with the scattering results (0.29, 0.73, 2.55 and 5.69 eV). We also employed the equation $\text{VAE} = 0.901 \times \text{VOE} - 2.550$ (in units of eV)³⁶ and estimated the energy of the σ_{CCl}^* resonance at 2.86 eV, in very good agreement with the scattering result of 3.00 eV. The parameters for the resonances of 2-chloroadenine are presented in Tab. I. The above mentioned values were computed by constraining the molecule to the C_s point group. Once the geometrical structure is fully optimised, the scaled VOEs become slightly stabilised (by no more than 0.1 eV), and thus we expect the computed resonances energies to behave similarly. Finally, the singly occupied molecular orbital of the DBS is also shown in Fig. 2, as obtained from an unrestricted HF calculation and extended basis set (see Sec. II). The binding energies obtained from the MP2 and CCSD(T) calculations are -11 meV and -31 meV, respectively.

The ion yield curves of the fragment anions observed from electron attachment to 2-chloroadenine are shown in Fig. 4. It appears that DEA occurs in two energy regions below 3 eV and between 4.5–7 eV. In comparison to DEA to adenine, the decomposition pattern is not very rich within the detection limit of the present experimental setup, and the interaction of low energy electrons with 2-chloroadenine leads to the formation of five anionic fragments detected at the experimental conditions at m/z 168 (taking into account ³⁵Cl), 133, 117, 35 and 45. The first four fragment anions are tentatively ascribed by stoichiometry to the $(\text{M}-\text{H})^-$, $(\text{M}-\text{HCl})^-$, $(\text{C}_5\text{HN}_4)^-$ and Cl^- , respectively. The structure of the fragment anion at m/z 45 is not obvious to us. In principle, it could be attributed to N_3H_3^- , however its

formation would require a very complex reaction, which is rather unlikely. Hence we cannot exclude that the fragment is generated from a minor decomposition of the compound at the hot filament leading to the formation of m/z 45.

The predominant negative ion, $(M-HCl)^-$, peaks at 0.2 eV and 1.0 eV and is generated from the concerted loss of H and Cl radicals, which most likely will recombine to form neutral stable molecule while the charge remains on the ring. Such reaction has been also observed in the case of 5-chlorouracil and 6-chlorouracil below 2 eV.³⁷ Surprisingly for 5-bromouracil it has been reported the loss of Br (and not HBr) leading to $(M-Br)^-$ ion.³⁸ This could be related to the difference of the binding energy of H-X (where X = Cl or Br), which is higher by 1.7 eV in the case of HCl and hence the formation of the HCl molecule is energetically more favourable.

The second predominant anion $(M-H)^-$ is formed from a loss of the hydrogen atom from the N9 position as shown from a studies of a series of methylated/deuterated purine bases,³⁹ which is also consistent with our calculations (see Fig. 2). The shape of the resonances in the ion yield curve is in a good agreement with the previous studies of DEA to adenine by the Innsbruck³⁴ and the Berlin group⁴⁰, while the position of the resonances is slightly shifted towards lower energy, which can be easily attributed to the stabilization effect of the chlorine atom.

The fragment anion Cl^- is generated from a direct single C-Cl bond cleavages. The chloride ion is generated at low energy range and visible via two overlapping structures with a peak maximum at 0.2 eV and 0.9 eV. It should be noted here that the peak with a maximum at 0.9 eV is almost three times higher than the 0.2 eV peak.

The remaining fragment m/z 117 ascribed to the $(C_5HN_4)^-$ ion, is generated with relatively small intensity. Its formation requires more complex reaction and proceeds via multiple bond cleavages, i.e., the C-H, C-Cl and C-NH₂ bonds. Such a product at m/z 117 has been previously observed from electron attachment to adenine⁴⁰ and attributed to the loss of NH₃ + H from the transient negative ion. In the case of DEA to 2-chloroadenine the reaction will either proceed via the loss of NH₃ + Cl or the loss of the neutral HCl molecule and the NH₂ radical. It is generated at three energy domains, namely at 1.9 eV, 5.2 eV and with some small intensity at around 6.6 eV. The maximum of the peaks is consistent with those for adenine, but with differences in the relative intensities. While in adenine the dominant structure was observed at around 5 eV, for the chloro-derivative the first peak is

the most abundant.

A rough comparison of the anionic yields of various fragments shows that the cross section of $(M-H)^-$, $(M-HCl)^-$ and Cl^- is more than one order of magnitude higher than the cross section of the $(C_5HN_4)^-$ anion as well as the fragment detected at m/z 45. Since the latter two fragment anions are produced with only minor intensity further discussion of the experimental data on the basis of theoretical results will mainly concern the three predominant anions, namely $(M-H)^-$, $(M-HCl)^-$ and Cl^- .

In order to induce the C–Cl bond breaking, the extra electron must locate at the anti-bonding σ_{CCl}^* orbital. Assuming a local dynamics, the vertical width of this anion state suggests a short-lived anion state (≈ 3 fs) that would not allow for significant vibrational relaxation, such that the direct occupation of this anion state does not seem to provide an efficient route for DEA. The longer-lived π^* anion states could in turn allow for vibration relaxation (including symmetry-breaking motion) thus coupling to the σ_{CCl}^* state in a geometry where the latter state could be lower in energy (therefore longer-lived) than in the ground state equilibrium geometry. The good matching between the two lower-lying π^* resonances and the observed peaks associated with the C–Cl cleavages suggest these DEA channels could arise from the π^*/σ_{CCl}^* indirect mechanism.⁴¹ The π_1^* resonance (0.29 eV) could account for the structures around 0.2 eV (Cl^- and $(M-HCl)^-$), while the π_2^* resonance (0.73 eV) would give rise to the peaks around 0.9 eV (Cl^-) and 1.0 eV ($(M-HCl)^-$). These channels are effective only below ~ 2 eV, and there seems to be no contribution from either the higher-lying π^* resonances or core-excited resonances. We do not expect the DBS to play a significant role in the formation of the Cl^- and $(M-HCl)^-$ anions, as the corresponding diffuse orbital has no overlap with the σ_{CCl}^* orbital. Zero-temperature G4(MP2) calculations support the threshold for Cl^- formation at 0.27 eV, which is compatible with the observed appearance energy. In the competing DEA channel, the chlorine atom would capture a hydrogen atom and give rise to the HCl neutral species. We found this reaction to be endothermic by only 0.18 eV in case the hydrogen comes from the N9 position and by 0.87 eV if it involves the amino group. Thus, the former reaction should account for the strongest 0.2 eV peak, while the 1.0 eV structure could in principle originate from both reactions.

Regarding the hydrogen elimination channel, the similarity between the curves of 2-chloroadenine and adenine^{34,40,42} suggests similar mechanisms in both molecules. The

DBS/ σ_{NH}^* coupling mechanism^{39,42,43} explains the most intense DEA signal of uracil⁴³ and adenine,⁴² and may operate here as well. Basically, the incoming electron is imprisoned into a vibrational Feshbach resonance (VFR) of the DBS, which is coupled to the dissociative σ_{NH}^* resonance. We can provide estimates for the VFR energies from the calculated DBS binding energy (-0.031 eV), obtained at the CCSD(T) level, the dissociation threshold of 0.67 eV, and the harmonic frequency for the N–H stretching mode (0.452 eV), assumed to be the same for the neutral molecule and the DBS. Dissociation from the $\nu = 1$ VFR (0.42 eV) would be energy-forbidden, although energy-allowed from the $\nu = 2$ VFR (0.87 eV). The latter energy is in good agreement with the observed 0.8 eV peak, thus supporting it would arise from the VFR. Higher-lying VFRs may also contribute in some extent above ~ 1 eV, albeit more weakly. In addition to coupling to the σ_{CCl}^* resonance, the π^* states may also couple to the σ_{NH}^* resonance and induce the N–H cleavage, thus accounting for the observed structures above ~ 1 eV. In view of the stabilisation of the π_2^* and π_3^* resonances in the chlorinated molecule, the corresponding structures in the DEA profile should also move correspondingly. Indeed, we observe this effect as the peaks appear around 1 and 1.8 eV (compared to 1.5 and 2.2 eV in adenine³⁴), despite our lower energy resolution. The shoulder around 1.8 eV is clearly distinguishable, and is assigned to the π_3^* resonance, while the π_2^* resonance should trigger off the hydrogen elimination close to 1 eV. However, contributions from both the $\nu = 2$ VFRs and the $\pi_2^*/\sigma_{\text{NH}}^*$ mechanism should account for the observed feature around 0.8 eV. The π_3^* resonance could also be responsible for the m/z 117 fragment observed at 2 eV, while the structure around 5 eV may originate from the π_4^* resonance.

V. SUMMARY

We investigated the anion spectra of 2-chloroadenine and its electron-induced fragmentation, under the interaction with electrons up to 12 eV. The resonance spectra was obtained from elastic scattering calculations, performed with the Schwinger multichannel method with pseudopotentials, and comprises four π^* and a σ_{CCl}^* shape resonances. We also performed scattering calculations for adenine, and the calculated anion spectrum shows improved agreement with experiment, in comparison to previous computational studies.

We found the π^* resonances effectively initiate dissociative electron attachment in 2-chloroadenine. These states may couple to the σ_{CCl}^* resonance and give rise to elimination

of chloride ion or hydrochloric acid. Furthermore, they may couple to the σ_{NH}^* state and induce hydrogen abstraction. Formation of a vibrational Feshbach resonance arising from the coupling of the dipole bound state to the σ_{NH}^* resonance accounts for the strongest signal in hydrogen elimination.

Our findings support that 2-chloroadenine decomposes into different reactive radicals when exposed to low-energy electrons. In particular, the neutral radical created upon cleavage of the C–Cl bond could attack the neighbouring nucleobases and/or backbone and increase the yields of strand breaks, when compared to the non-chlorinated adenine. The present results thus support 2-chloroadenine as a potential sensitiser to be considered in future radiolytic studies.

ACKNOWLEDGMENTS

F. K. and M. T. do N. V. acknowledge financial support from Fundação de Amparo à Pesquisa do Estado de São Paulo (FAPESP). M. T. do N. V. also acknowledges support from Conselho Nacional de Desenvolvimento Científico e Tecnológico (CNPq). This work employed computational resources from LCCA-USP and CENAPAD-SP. J. K. acknowledges support from Polish Ministry of Science and Higher Educations.

REFERENCES

- ¹B. Boudaïffa, P. Cloutier, D. Hunting, M. A. Huels, and L. Sanche, *Science* **287**, 1658 (2000).
- ²H. Abdoul-Carime, M. A. Huels, E. Illernberger, and L. Sanche, *J. Am. Chem. Soc.* **123**, 5354 (2001).
- ³P. Wardman, *Clin. Oncol.*, **19**, 397 (2007).
- ⁴L. Chomicz, J. Rak, and P. Storoniak, *J. Phys. Chem. B* **116**, 5612 (2012).
- ⁵L. Chomicz, J. Leszczynski, and J. Rak, *J. Phys. Chem. B* **117**, 8681 (2013).
- ⁶L. Chomicz, A. Furmanchuk, J. Leszczynski, and J. Rak, *Phys. Chem. Chem. Phys.* **16**, 6568 (2014).
- ⁷M. Wieczór, P. Wityk, J. Czub, L. Chomicz, and J. Rak, *Chem. Phys. Lett.* **595-596**, 133 (2014).

- ⁸Y. Park, K. Polska, J. Rak, J. R. Wagner, and L. Sanche, *J. Phys. Chem. B* **116**, 9676 (2012).
- ⁹S. Tonzani and C. H. Greene, *J. Chem. Phys.* **124**, 054312 (2006).
- ¹⁰C. Winstead and V. McKoy, *J. Chem. Phys.* **125**, 244302 (2006).
- ¹¹A. Dora, L. Bryjko, T. van Mourik, and J. Tennyson, *J. Chem. Phys.* **136**, 024324 (2012).
- ¹²K. Aflatooni, G. Gallup, and P. Burrow, *J. Phys. Chem. A* **102**, 6205 (1998).
- ¹³M. H. F. Bettega, A. P. P. Natalense, M. A. P. Lima, and L. G. Ferreira, *Int. J. Quantum Chem.* **60**, 821 (1996).
- ¹⁴F. Kossoski, M. H. F. Bettega, and M. T. do N. Varella, *J. Chem. Phys.* **140**, 024317 (2014).
- ¹⁵T. H. Dunning, Jr., *J. Chem. Phys.* **53**, 2823 (1970).
- ¹⁶G. B. Bachelet, D. R. Hamann, and M. Schlüter, *Phys. Rev. B* **26**, 4199 (1982).
- ¹⁷M. W. Schmidt, K. K. Baldridge, J. A. Boatz, S. T. Elbert, M. S. Gordon, J. H. Jensen, S. Koseki, N. Matsunaga, K. A. Nguyen, S. J. Su, T. L. Windus, M. Dupuis, and J. A. Montgomery, *J. Comput. Chem.* **14**, 1347 (1993).
- ¹⁸K. Takatsuka and V. McKoy, *Phys. Rev. A* **24**, 2473 (1981); **30**, 1734 (1984).
- ¹⁹M. H. F. Bettega, L. G. Ferreira, and M. A. P. Lima, *Phys. Rev. A* **47**, 1111 (1993).
- ²⁰J. S. dos Santos, R. F. da Costa, and M. T. do N. Varella, *J. Chem. Phys.* **136**, 084307 (2012).
- ²¹R. F. da Costa, M. T. do N. Varella, M. H. F. Bettega, and M. A. P. Lima, *Eur. Phys. J. D* **69**, 159 (2015).
- ²²C. W. Bauschlicher, Jr., *J. Chem. Phys.* **72**, 880 (1980).
- ²³W. Zierkiewicz, L. Komorowski, D. Michalska, J. Cerny, P. Hobza, *J Phys Chem B* **112**, 16734 (2008).
- ²⁴F. Kossoski and M. H. F. Bettega, *J. Chem. Phys.* **138**, 234311 (2013).
- ²⁵E. M. de Oliveira, R. F. da Costa, S. d'A. Sanchez, A. P. P. Natalense, M. H. F. Bettega, M. A. P. Lima and M. T. do N. Varella, *Phys. Chem. Chem. Phys.* **15**, 1682 (2013).
- ²⁶M. J. Frisch, G. W. Trucks, H. B. Schlegel, G. E. Scuseria, M. A. Robb, J. R. Cheeseman, G. Scalmani, V. Barone, B. Mennucci, G. A. Petersson, H. Nakatsuji, M. Caricato, X. Li, H. P. Hratchian, A. F. Izmaylov, J. Bloino, G. Zheng, J. L. Sonnenberg, M. Hada, M. Ehara, K. Toyota, R. Fukuda, J. Hasegawa, M. Ishida, T. Nakajima, Y. Honda, O. Kitao, H. Nakai, T. Vreven, J. A. Montgomery, Jr., J. E. Peralta, F. Ogliaro, M. Bearpark,

- J. J. Heyd, E. Brothers, K. N. Kudin, V. N. Staroverov, R. Kobayashi, J. Normand, K. Raghavachari, A. Rendell, J. C. Burant, S. S. Iyengar, J. Tomasi, M. Cossi, N. Rega, J. M. Millam, M. Klene, J. E. Knox, J. B. Cross, V. Bakken, C. Adamo, J. Jaramillo, R. Gomperts, R. E. Stratmann, O. Yazyev, A. J. Austin, R. Cammi, C. Pomelli, J. W. Ochterski, R. L. Martin, K. Morokuma, V. G. Zakrzewski, G. A. Voth, P. Salvador, J. J. Dannenberg, S. Dapprich, A. D. Daniels, Ö. Farkas, J. B. Foresman, J. V. Ortiz, J. Cioslowski, and D. J. Fox, Gaussian, Inc., Wallingford CT, 2009.
- ²⁷P. Skurski, M. Gutowski, and J. Simons, *Int. J. Quant. Chem.* **80**, 1024 (2000).
- ²⁸C. M. Marian, *J. Chem. Phys.* **122**, 104314 (2005).
- ²⁹I. Nenner and G. J. Schulz, *J. Chem. Phys.* **62**, 1747 (1975).
- ³⁰C. Winstead and V. McKoy, *Phys. Rev. Lett.* **98**, 113201 (2007).
- ³¹Pseudoresonances are unphysical features that may arise in the computed cross sections when open excited states of the target are not included in the P projection operator. In this case, the incoming electron has enough energy to excite the target state, but it cannot escape into the excitation channel that is disregarded in the calculation. Therefore the system must undergo a de-excitation so the electron can escape into the elastic channel, giving rise to an artificial long-lived anion state (pseudoresonance).
- ³²E. M. de Oliveira, M. A. P. Lima, M. H. F. Bettega, S. d'A Sanchez, R. F. da Costa, and M. T. do N. Varella, *J. Chem. Phys.* **132**, 204301 (2010).
- ³³E. M. de Oliveira, S. d'A Sanchez, M. H. F. Bettega, A. P. P. Natalense, M. A. P. Lima, and M. T. do N. Varella, *Phys. Rev. A* **86**, 20701 (2012).
- ³⁴D. Huber, M. Beikircher, S. Denifl, F. Zappa, S. Matejcik, A. Bacher, V. Grill, T. D. Märk, and P. Scheier, *J. Chem. Phys.* **125**, 084304 (2006).
- ³⁵S. W. Staley and J. T. Strnad, *J. Chem. Phys.* **98**, 116 (1994).
- ³⁶K. Aflatooni, G. A. Gallup, and P. D. Burrow, *J. Phys. Chem. A* **104**, 7359 (2000).
- ³⁷S. Denifl, S. Matejcik, S. Ptasinska, B. Gstir, M. Probst, P. Scheier, E. Illenberger, and T. D. Märk, *J. Chem. Phys.* **120**, 704 (2004).
- ³⁸R. Abouaf, J. Pommier, and H. Dunet, *Int. J. Mass Spectrom.* **226**, 397 (2003).
- ³⁹S. Denifl, P. Sulzer, D. Huber, F. Zappa, M. Probst, T. D. Märk, P. Scheier, N. Injan, J. Limtrakul, R. Abouaf, and H. Dunet, *Angew. Chem. Int. Ed. Engl.* **46**, 5238 (2007).
- ⁴⁰S. Gohlke, H. Abdoul-Carime, and E. Illenberger, *Chem. Phys. Lett.* **380**, 595 (2003).

- ⁴¹H. Hotop, M.-W. Ruf, M. Allan and I. I. Fabrikant, *Adv. At., Mol., Opt. Phys.*, **49**, 85 (2003).
- ⁴²K. Aflatooni, A. M. Scheer, and P. D. Burrow, *J. Chem. Phys.* **125**, 054301 (2006).
- ⁴³A. Scheer, K. Aflatooni, G. Gallup, and P. Burrow, *Phys. Rev. Lett.* **92**, 068102 (2004).

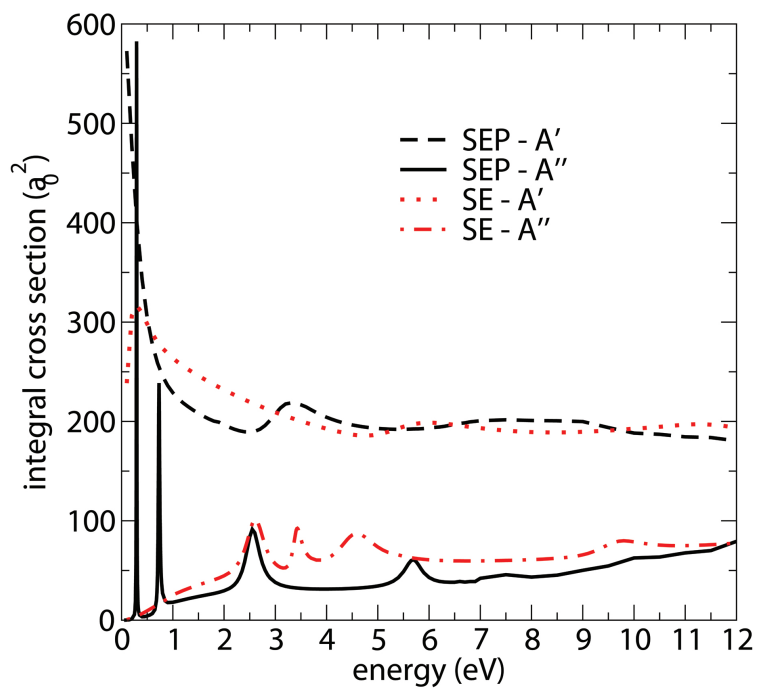


FIG. 1. Contributions from the A' and A'' components to the elastic integral cross section of 2-chloroadenine, computed at the SE and SEP approximations.

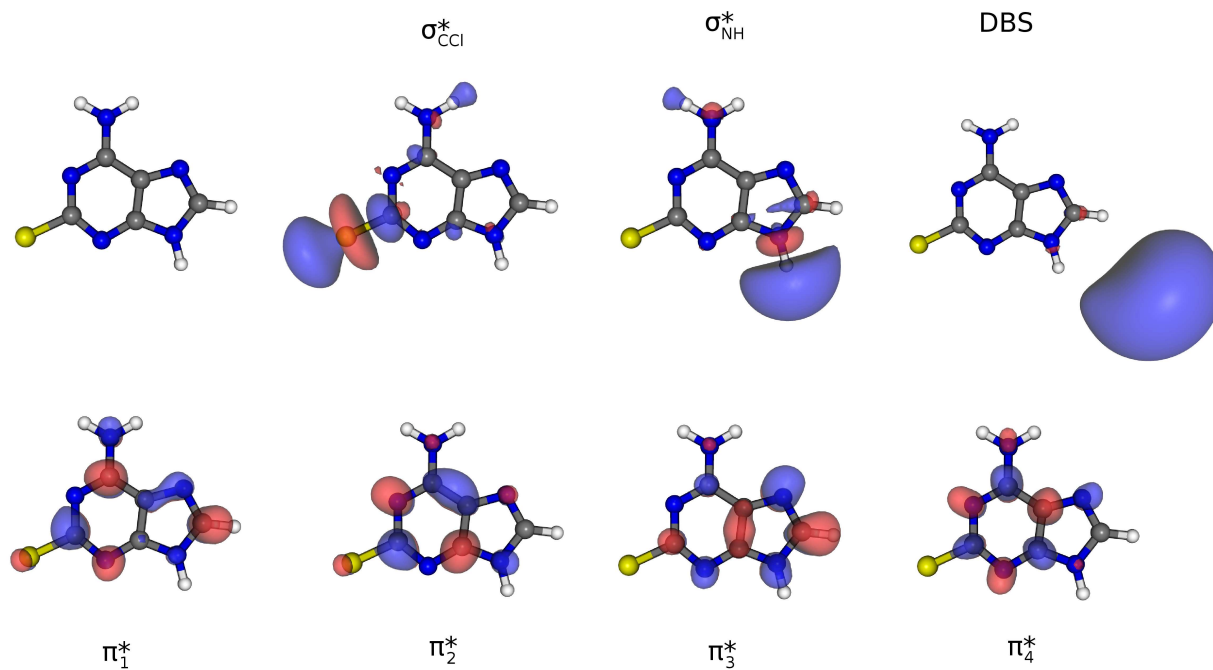


FIG. 2. Upper part, from left to right: structure of 2-chloroadenine (with the following correspondence between atoms and colours: Cl (yellow), N (blue), C (grey) and H (white)), σ_{CCl}^* and σ_{NH}^* virtual orbitals and DBS singly occupied orbital. Bottom part, from left to right: π_1^* , π_2^* , π_3^* and π_4^* virtual orbitals. The plots for the valence and the dipole-bound orbitals correspond to the isovalues of 0.04 and 0.01 a.u., respectively.

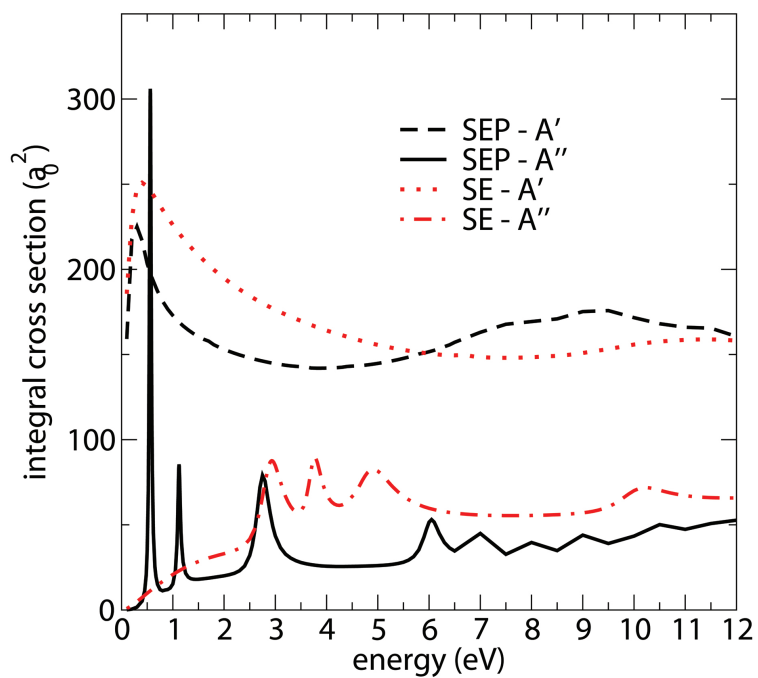


FIG. 3. Contributions from the A' and A'' components to the elastic integral cross section of adenine, computed at the SE and SEP approximations.

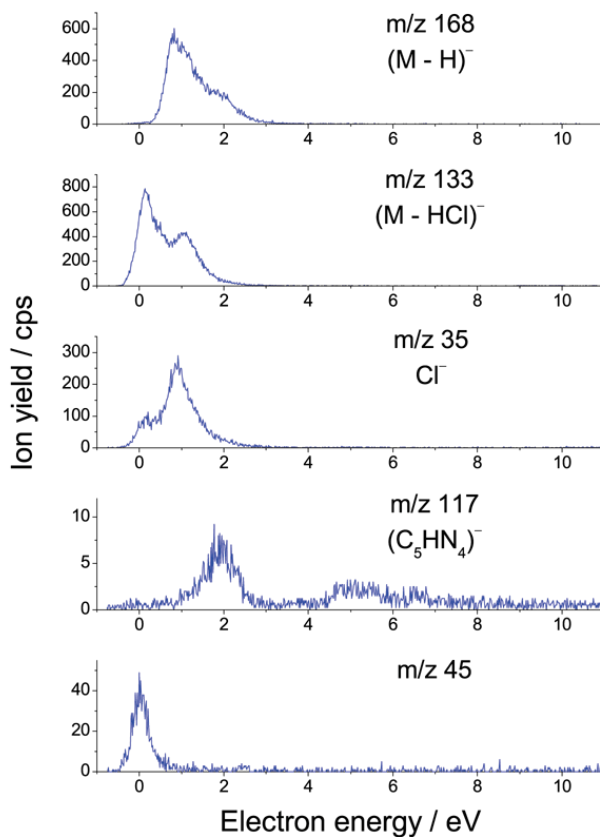


FIG. 4. Ion yield curves for the dissociative electron attachment to 2-chloroadenine resulting in the formation of m/z 168 ($M-H$)⁻, m/z 133 ($M-HCl$)⁻, m/z 35 (Cl)⁻, m/z 117 (C_5HN_4)⁻ and m/z 45.

TABLE I. Energies and widths (the latter in parenthesis) of the shape resonances of 2-chloroadenine and adenine (in units of eV). It is shown results according to our SMCPP scattering calculations and scaled VOs, as well as existing results from ET data of Afatooni *et al.*,¹² SMC calculations of Winstead and McKoy,¹⁰ R-matrix SEP and u-CC calculations of Dora *et al.*,¹¹ and R-matrix one-electron model calculations of Tonzani and Greene.⁹

2-chloroadenine	π_1^*	π_2^*	π_3^*	π_4^*	σ_{CCl}^*
SMCPP	0.29 (0.0084)	0.73 (0.030)	2.55 (0.32)	5.69 (0.43)	3.00 (1.16)
Scaled VOs	0.61	1.12	2.01	5.04	2.86
Adenine	π_1^*	π_2^*	π_3^*	π_4^*	
SMCPP	0.56 (0.045)	1.12 (0.029)	2.72 (0.31)	6.02 (0.39)	
ET data ¹²	0.54	1.36	2.17		
SMC ¹⁰	1.1	1.8	4.1		
R-matrix (SEP) ¹¹	1.30 (0.14)	2.12 (0.09)	3.12 (0.28)	7.07 (0.24)	
R-matrix (u-CC) ¹¹	1.58 (0.22)	2.44 (0.14)	4.38 (0.67)	7.94 (0.57)	
R-matrix ⁹	2.4 (0.2)	3.2 (0.2)	4.4 (0.3)	9.0 (0.5)	